

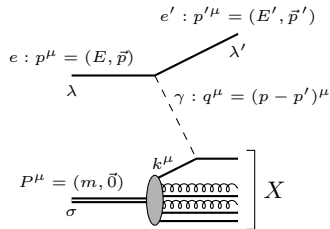
Review on Color Glass Condensate (CGC) results.

F. Cougoulic (Jagiellonian University)

AGH - November 14, 2025.

A short introduction to the CGC framework - Prototype process: DIS

“The Diagram”:



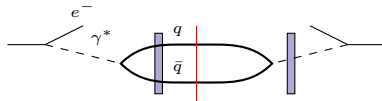
Kinematic invariants

$$Q^2 \equiv -q^2, \quad (\gamma\text{-virtuality})$$

$$x_B \equiv \frac{Q^2}{2P \cdot q} = \frac{Q^2}{\hat{s} + Q^2 - m^2} \quad (\text{Bjorken-}x),$$

$$y \equiv \frac{E - E'}{E}, \quad (\text{Inelasticity})$$

Factorization in the CGC framework: study the small- x behavior \rightarrow High Energy limit.



$$\sigma_{T,L}^{\gamma^* p}(x, Q^2) = \sigma_0 \int d^2 \underline{r} \int_0^1 dz |\Psi_{T,L}(\underline{r}, z, Q^2)| \left[1 - S_{\underline{r}}^{(\eta = \ln 1/x)} \right] \quad (2)$$

A short introduction to the CGC framework - Scattering in the high energy limit.

Taking the HE limit: consider the scattering of a probe on some (localized) external field,

- S-matrix $S_{\beta\alpha} = \langle \beta_{out} | \alpha_{in} \rangle$ (finite energy).
- Evolution operator U write $S_{\beta\alpha} = \langle \beta_{in} | U(\infty, -\infty) | \alpha_{in} \rangle = \langle \beta_{in} | T e^{i \int d^4x \mathcal{L}_{int}(x)} | \alpha_{in} \rangle$.
- Apply a boost in the longitudinal direction to the states α, β :
 $|\alpha_{in}\rangle \rightarrow e^{-i w K^3} |\alpha_{in}\rangle$, and extract the limit of infinite boost of the amplitude.

Eikonal scattering: as a consequence to the infinite boost limit,

- Support of the external field is contracted: $L \rightarrow 0$;
and its configuration is frozen ("glass"): $\tau_{int} \ll \tau_{probe}$.
- Component of the external gauge field are ordered in [eikonal](#)ity: $A^\pm \gg A_\perp \gg A^\mp$
- Wave function is evolved from $-\infty$ to 0, then the scattering is a phase rotation encoded into [Wilson lines](#).

Beyond Eikonal, Sub-Eikonal, next-to-eikonal, ... : consists of relaxing the above limits.

A short introduction to the CGC framework: JIMWLK equation

Where is the dynamics?

Expectation of an operator made of Wilson Lines (WL) at a given rapidity

$$\langle \hat{O}_\alpha \rangle_Y = \frac{\int \mathcal{D}\alpha \hat{O} W_Y[\alpha]}{\int \mathcal{D}\alpha W_Y[\alpha]}$$

Annotations:

- Rapidity Y (red arrow)
- $\alpha \equiv$ the large component of the gauge field (red text)
- target weight functional (blue text)
- target average (green text)

$$\int \mathcal{D}\alpha W_Y[\alpha] = 1$$

Evolution $Y \rightarrow Y + \delta Y$

$$\partial_Y W_Y[\alpha] = H_{JIMWLK} \cdot W_Y[\alpha] \quad (3)$$

Evolution Hamiltonian

$$H_{JIMWLK} \equiv \frac{\alpha_s}{2\pi^2} \int d^2 \underline{x} d^2 \underline{y} d^2 \underline{z} \frac{(\underline{x} - \underline{z}) \cdot (\underline{y} - \underline{z})}{(\underline{x} - \underline{z})^2 (\underline{y} - \underline{z})^2} (2U_{\underline{z}} - U_{\underline{x}} - U_{\underline{y}})^{ba} (ig)^{-2} \frac{\delta}{\delta \alpha^a(x^- < 0, \underline{x})} \frac{\delta}{\delta \alpha^b(y^- > 0, \underline{y})} \quad (4)$$

⇒ Acting on the dipole operator $S = \text{tr } VV^\dagger$ and taking the large N_c limits yields BK equation.

Initial condition for the evolution:

- GBW: the dipole reads $S^{GBW}(r_\perp) = \exp(-r_\perp^2 Q_s^2)$
- MV: the dipole reads $S^{MV}(r_\perp) = \exp(-r_\perp^2 Q_s^2 \ln \frac{1}{r_\Lambda})$

An overview of recent developments

Accuracy of CGC calculations

- Next-to-leading order
- Beyond Eikonal approximation
- HE evolution and Collinear evolution

Phenomenology using the CGC

- Many dijets
- Meson production

Disclaimer: This is not an exhaustive review.

Part 1: Improving the accuracy of CGC calculations

Next-to-leading order: JIMWLK kernels

A. Kovner, M. Lublinsky, Y. Mulian - JHEP 08 (2014) 114 / JHEP 05 (2017) 097

Evolution of an operator \hat{O} over a rapidity interval δY :

$$\hat{O} \longrightarrow e^{-\delta Y H_{JIMWLK}} \hat{O}, \quad \text{where } H_{JIMWLK} = H_{JIMWLK}^{LO}(\alpha_s) + H_{JIMWLK}^{NLO}(\alpha_s^2) + \dots \quad (5)$$

$$H_{JIMWLK}^{LO} = \frac{\alpha_s}{2\pi^2} \int_{\mathbf{x}, \mathbf{y}, \mathbf{z}} \frac{X \cdot Y}{X^2 Y^2} \left[J_L^a(\mathbf{x}) J_L^a(\mathbf{y}) + J_R^a(\mathbf{x}) J_R^a(\mathbf{y}) - 2 J_L^a(\mathbf{x}) S_A^{ab}(\mathbf{z}) J_R^b(\mathbf{y}) \right]. \quad (6)$$

$$\begin{aligned} H_{JIMWLK}^{NLO} = & \int_{\mathbf{x}, \mathbf{y}, \mathbf{z}} K_{JSJ}(\mathbf{x}, \mathbf{y}, \mathbf{z}) \left[J_L^a(\mathbf{x}) J_L^a(\mathbf{y}) + J_R^a(\mathbf{x}) J_R^a(\mathbf{y}) - 2 J_L^a(\mathbf{x}) S_A^{ab}(\mathbf{z}) J_R^b(\mathbf{y}) \right] \\ & + \int_{\mathbf{x}, \mathbf{y}, \mathbf{z}, \mathbf{z}'} K_{JSSJ}(\mathbf{x}, \mathbf{y}, \mathbf{z}, \mathbf{z}') \left[f^{abc} f^{def} J_L^a(\mathbf{x}) S_A^{be}(\mathbf{z}) S_A^{cf}(\mathbf{z}') J_R^d(\mathbf{y}) - N_c J_L^a(\mathbf{x}) S_A^{ab}(\mathbf{z}) J_R^b(\mathbf{y}) \right] \\ & + \int_{\mathbf{x}, \mathbf{y}, \mathbf{z}, \mathbf{z}'} K_{q\bar{q}}(\mathbf{x}, \mathbf{y}, \mathbf{z}, \mathbf{z}') \left[2 J_L^a(\mathbf{x}) \text{tr}[S^\dagger(\mathbf{z}) t^a S(\mathbf{z}') t^b] J_R^b(\mathbf{y}) - J_L^a(\mathbf{x}) S_A^{ab}(\mathbf{z}) J_R^b(\mathbf{y}) \right] \\ & + \int_{\mathbf{w}, \mathbf{x}, \mathbf{y}, \mathbf{z}, \mathbf{z}'} K_{JJSSJ}(\mathbf{w}, \mathbf{x}, \mathbf{y}, \mathbf{z}, \mathbf{z}') f^{acb} \left[J_L^d(\mathbf{x}) J_L^e(\mathbf{y}) S_A^{dc}(\mathbf{z}) S_A^{eb}(\mathbf{z}') J_R^a(\mathbf{w}) \right. \\ & \left. - J_L^a(\mathbf{w}) S_A^{cd}(\mathbf{z}) S_A^{be}(\mathbf{z}') J_R^d(\mathbf{x}) J_R^e(\mathbf{y}) + \frac{1}{3} (J_L^c(\mathbf{x}) J_L^b(\mathbf{y}) J_L^a(\mathbf{w}) - J_R^c(\mathbf{x}) J_R^b(\mathbf{y}) J_R^a(\mathbf{w})) \right] \\ & + \int_{\mathbf{w}, \mathbf{x}, \mathbf{y}, \mathbf{z}} K_{JJSJ}(\mathbf{w}, \mathbf{x}, \mathbf{y}, \mathbf{z}) f^{bde} \left[J_L^d(\mathbf{x}) J_L^e(\mathbf{y}) S_A^{ba}(\mathbf{z}) J_R^a(\mathbf{w}) \right. \\ & \left. - J_L^a(\mathbf{w}) S_A^{ab}(\mathbf{z}) J_R^d(\mathbf{x}) J_R^e(\mathbf{y}) + \frac{1}{3} (J_L^d(\mathbf{x}) J_L^e(\mathbf{y}) J_L^b(\mathbf{w}) - J_R^d(\mathbf{x}) J_R^e(\mathbf{y}) J_R^b(\mathbf{w})) \right]. \end{aligned} \quad (7)$$

- NLO Hamiltonian has rich Lorentz and color structure: RG / DGLAP / ...
- Still lacking a numerical implementation.

Next-to-leading order: JIMWLK kernels - relative to BK progress

Status of the numerical implementations

Forefront (unpolarized - eikonal)

Personal bias: (polarized)

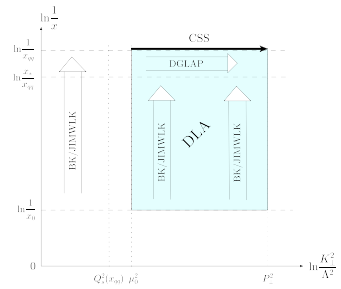
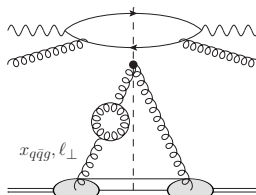
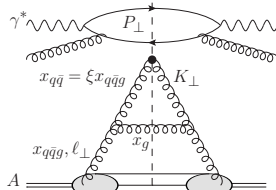
@eik	BK	JIMWLK	@sub-eik	Large- N_C	Large- $N_c \& N_f$	All- N_c
LO	✓	✓	LO	✓	✓	✗
r.c.	✓	✓	r.c.	✗	✗	✗
k.c.	✓	✗	NLO	✗	✗	✗
NLO	✓/✗	✗				
N^2LO	✗	✗				

There is still a lot of fun to have!

Next-to-leading order: Evolution of gluon TMD at small- x

P. Caucal and E. Iancu - Phys. Rev. D 111 (2025) 7, 074008

- Compute NLO correction to the production of pair of hard jets in DIS.
- NLO corrections include the JIMWLK evolution but also the DGLAP/CSS evolution.
- Expect all three type of evolution to be relevant for $P_\perp \gg K_\perp \gg Q_s(x)$.
Propose a framework to encompass all three evolution.
- Confirm: Sudakov effect can be resummed according to CSS-eqs for the TMD.
- The dijet relative momentum P_\perp sets the scales for both CSS-eqs (specific trajectory in CSS $\mu - \xi$ plane).



Next-to-leading order: with/without Sudakov

P. Caucal, F. Salazar, B. Schenke, T. Stobel, R. Venugopalan - Phys. Rev. Lett. 132 (2024) 8, 081902

- Back-to-back dijet in DIS at NLO within the CGC framework
- Result expressed as:

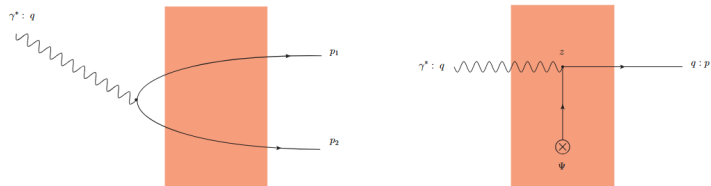
$$\begin{aligned}
 \left\langle d\sigma_{\text{LO}}^{(0),\lambda,\text{b2b}} + \alpha_s d\sigma_{\text{NLO}}^{(0),\lambda,\text{b2b}} \right\rangle_{\eta_f} = & \mathcal{H}_{\text{LO}}^{0,\lambda} \int \frac{d^2 B_\perp}{(2\pi)^2} \int \frac{d^2 r_{bb'}}{(2\pi)^2} e^{-i\mathbf{q}_\perp \cdot \mathbf{r}_{bb'}} \hat{G}_{\eta_f}^0(\mathbf{r}_{bb'}, \mu_0) \left\{ 1 + \frac{\alpha_s(\mu_R)}{\pi} \left[\underbrace{-\frac{N_c}{4} \ln^2 \left(\frac{P_\perp^2 r_{bb'}^2}{c_0^2} \right)}_{\text{Sudakov double log}} \right. \right. \\
 & \left. \left. - s_L \ln \left(\frac{P_\perp^2 r_{bb'}^2}{c_0^2} \right) + \beta_0 \ln \left(\frac{\mu_R^2 r_{bb'}^2}{c_0^2} \right) + \frac{N_c}{2} f_1^\lambda(\chi, z_1, R, \eta_f) + \frac{1}{2N_c} f_2^\lambda(\chi, z_1, R) \right] \right\} \\
 & + \frac{\alpha_s(\mu_R)}{\pi} \mathcal{H}_{\text{LO}}^{0,\lambda} \int \frac{d^2 B_\perp}{(2\pi)^2} \int \frac{d^2 r_{bb'}}{(2\pi)^2} e^{-i\mathbf{q}_\perp \cdot \mathbf{r}_{bb'}} \hat{h}_{\eta_f}^0(\mathbf{r}_{bb'}, \mu_0) \left\{ \frac{N_c}{2} [1 + \ln(R^2)] - \frac{1}{2N_c} \ln(z_1 z_2 R^2) \right\}. \quad (11)
 \end{aligned}$$

- Up to correction of order q_\perp^2/P_\perp^2 , Q_s^2/P_\perp^2 .
- \hat{G}^0 - unpol WW gluon TMD / \hat{h} - linearly pol WW gluon TMD
- Correct Sudakov implies the introduction of lifetime ordering for the action of the JIMWLK kernel on the WW TMD.

Beyond Eikonal approximation: Relations to TMDs

T. Altinoluk, G. Beuf and S. Mulani - PoS DIS2024 (2025) 077

- Compute the SIDIS cross-section

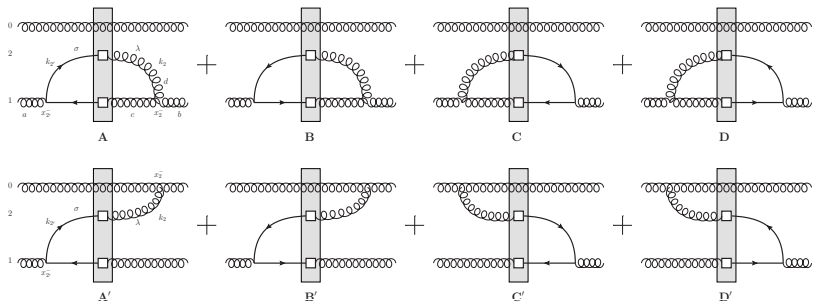


- Beyond eikonal approximation in the CGC. Inclusion of the quark background field.
- Directly relates to the (valence) quark TMD:
 $\propto \langle P_{tar} | \bar{\Psi}(z^+, b_\perp) \gamma^- V^\dagger[\infty, z^+; b_\perp] V[\infty, 0; 0_\perp] \Psi(0^+, 0_\perp) | P_{tar} \rangle$
- To be contrasted to the eikonal contribution where one recovers the sea quark TMD.

Beyond Eikonal approximation: Spin physics

J. Borden, Y. Kovchegov, M. Li - JHEP 09 (2024) 037

- Helicity evolution at small- x involves sub-eikonal operators.
- Evolution equations are double logarithmic $\int \frac{dz}{z} \int \frac{d^2 w}{(w-x_i)^2}$
- Modifies previous results [JHEP 07 (2022) 095] in the Veneziano large N_c & N_f limit.
- Involves fermion-boson $\langle \bar{\psi}(y) a^\mu(x) \rangle$ propagators in a background / Transition operators.
- Relevant for flavor singlet evolution and flavor non-singlet.



Beyond Eikonal approximation: Spin physics

J. Borden, Y. Kovchegov, M. Li - JHEP 09 (2024) 037

- Agreement with existing 3-loop splitting functions for ΔP_{qq} , ΔP_{gg} in \overline{MS} and (BER IRE).
- ΔP_{qg} and ΔP_{gq} differs at $\mathcal{O}(\alpha_s)$ with \overline{MS} . Attributed to scheme difference.

Prediction for the polarized splitting function at 4-loops at small- x .

$$\Delta P_{qq}^{(3)}(x) = \left(\frac{\alpha_s N_c}{4\pi}\right)^4 \frac{1}{720} \left(5 - 748 \frac{N_f}{N_c} + 80 \frac{N_f^2}{N_c^2}\right) \ln^6 \frac{1}{x}, \quad (8a)$$

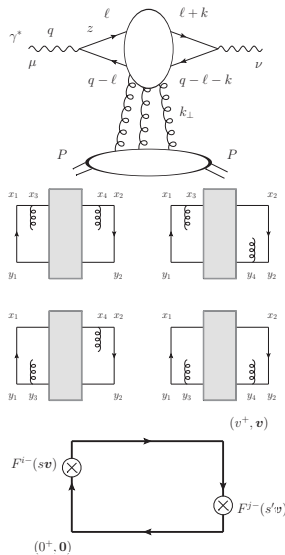
$$\Delta P_{qG}^{(3)}(x) = - \left(\frac{\alpha_s N_c}{4\pi}\right)^4 \frac{1}{360} \frac{N_f}{N_c} \left(1213 - 224 \frac{N_f}{N_c}\right) \ln^6 \frac{1}{x}, \quad (8b)$$

$$\Delta P_{Gq}^{(3)}(x) = \left(\frac{\alpha_s N_c}{4\pi}\right)^4 \frac{1}{360} \left(1213 - 224 \frac{N_f}{N_c}\right) \ln^6 \frac{1}{x}, \quad (8c)$$

$$\Delta P_{GG}^{(3)}(x) = \left(\frac{\alpha_s N_c}{4\pi}\right)^4 \frac{1}{180} \left(1984 - 549 \frac{N_f}{N_c} + 20 \frac{N_f^2}{N_c^2}\right) \ln^6 \frac{1}{x}. \quad (8d)$$

HE evolution and Collinear evolution: finite length operators

R. Boussarie and Y. Mehtar-Tani - JHEP 07 (2022) 080



- Consider DIS cross section
- Aim: factorization valid in both the Bjorken limit ($Q^2 \rightarrow \infty$ while x_{Bj} finite) and the Regge limit ($s \rightarrow \infty$ equiv. $x_{Bj} \rightarrow 0$ while Q^2 finite)
- Consider the hadronic tensor $W^{\mu\nu}$ where the the propagators are in the bg of the *eikonal* gauge field $A^-(x^2, x_\perp)$.
- Beyond the usual approximation $\tau_{q\bar{q}} \gg \tau_{int}$
- Medium length L^+ identified by the very first and very last interaction
- $A^-(x^+, y_\perp) - A^-(x^-, x_\perp) \rightarrow \int_{x_\perp}^{y_\perp} dw^i F^{i-}(x^+, w_\perp)$
- Finite length operators: box with two field strength tensors insertion on transverse links.
- Limiting cases: Bjorken limit $v_\perp \rightarrow 0_\perp$ gives collinear pdf, Regge limit gives dipole cross section.

HE evolution and Collinear evolution: DGLAP summation in JIMWLK evolution

A. Kovner, M. Lublinsky, V. Skokov, Z. Zhao - JHEP 07 (2024) 148

- Starting from the NLO JIMWLK Hamiltonian, study the the transverse logs associated to β_0 .
- “*Not all that is β_0 is β -function*”
- $2\beta_0$ contribution in front of $\ln \mu_{\overline{MS}}^2$. Half of it is associated to DGLAP-like evolution (low-x pole is subtracted), as opposed to the running coupling.
- Implemented into JIMWLK hamiltonian by introducing *dressed* Wilson lines \mathbb{S}_Q^{ab} to order α_s with resolution Q :

$$\begin{aligned} \mathbb{S}_Q^{ab}(\mathbf{z}) = & S^{ab}(\mathbf{z}) + \frac{\alpha_s}{2\pi^2} \int_0^1 \frac{d\xi}{\xi_+(1-\xi)_+} (\xi^2 + (1-\xi)^2 + \xi^2(1-\xi)^2) \\ & \times \int_{\mu^{-1} < |Z| < Q^{-1}} \frac{d^2Z}{Z^2} \left[D^{ab}(\mathbf{z} + (1-\xi)Z, \mathbf{z} - \xi Z) - N_c S^{ab}(\mathbf{z}) \right] \end{aligned} \quad (9)$$

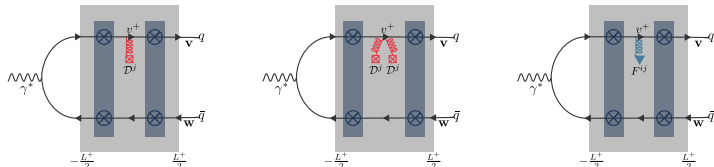
- HE evolution for dressed WL \mathbb{S}_Q^{ab} , which solve DGLAP (resumming $\ln X_\perp^2 Q^2$) while $\ln X_\perp^2 \mu_{\overline{MS}}^2$ is associated to r.c.

Part 2: Phenomenology using the CGC

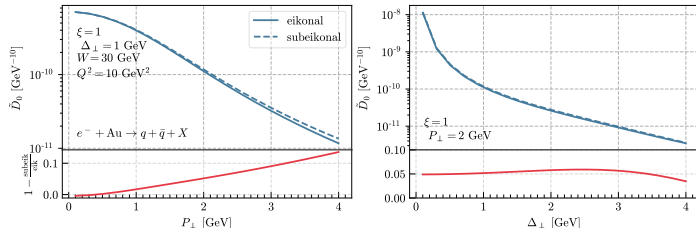
Many dijets: Dijet production at Next-to-eikonal

P. Agostini, T. Altinoluk and N. Armesto - JHEP 07 (2024) 137

- Dijet production in DIS
- Computation at next-to-eikonal, introduce decorated WLs. Contains field insertion beyond the large component of the gauge field.



- Beyond the shockwave approximation: splitting inside the shock, finite length.
- Evaluated in the dilute limit: WL expanded to order $\mathcal{O}(g^2)$, for both next-to-eikonal dipole and quadrupole.



Many dijets: probing WW helicity TMD

Y. Kovchegov and M. Li - JHEP 08 (2025) 206

- Dijet production in polarized DIS
- Computation at sub-eikonal accuracy using polarized WLs.
- Contains contribution of the $\gamma \rightarrow q\bar{q}$ splitting within the shock-wave (beyond sw approximation).
- In the back-to-back kinematic limit probes the Weizsäcker-Williams gluon helicity TMD.

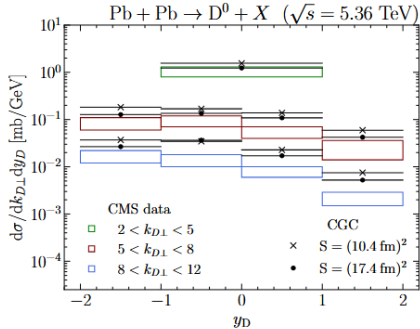
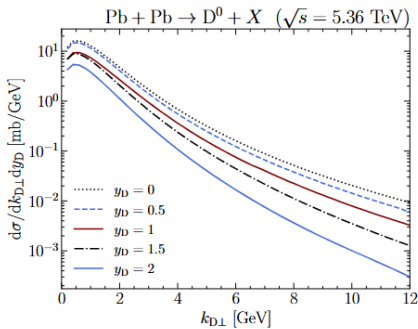
$$\sum_{\lambda=\pm 1} \lambda z(1-z) \frac{d\sigma^{\gamma^* p \rightarrow q\bar{q} X}}{d^2 p \, d^2 \Delta \, dz} \approx -\frac{2 \alpha_s \alpha_{EM} Z_f^2}{s} \left[z^2 + (1-z)^2 \right] \frac{p_T^2 - a_f^2}{(p_T^2 + a_f^2)^2} g_{1L}^{GWW} \left(x \approx \frac{p_T^2}{s}, \Delta_T^2 \right). \quad (10)$$

- Study the small- x evolution of this TMD at DLA in the large N_c -limit.
- Outside the saturation region, show that $g_{1L}^{GWW}(x, k_\perp^2) \sim g_{1L}^{G\,dip}(x, k_\perp^2)$.
Related to the evolution of the same operator G_2 .
- Can be used to further constrain the proton spin at low- x .

Meson production: Inclusive D^0 production in UPC

[P. Gimeno-Estivill, T. Lappi and H. Mantysaari - Phys.Rev.D 111 (2025) 11, 114036]

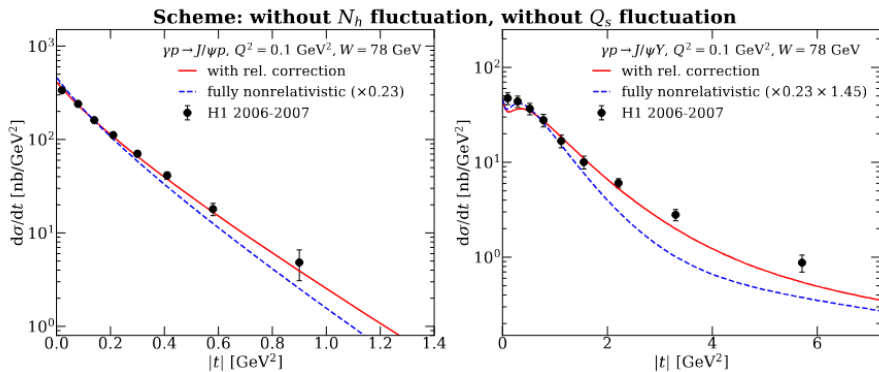
- Compute the cross section for $d\sigma^{A+A \rightarrow D^0 + X} / dy_D d^2 k_{D\perp}$ in UPCs
- Partonic process $\gamma + A_\mu^{cl} \rightarrow q\bar{q}$.
- **Probe the dipole $D = \langle \text{tr } VV^\dagger \rangle$** [antiquark integrated out, thus quadrupole collapses]
- Dipole evolved according to rcBK from an initial condition MV^e fitted to HERA-data
- Compared to CMS-data.



Meson production: Coherent vs incoherent in exclusive J/ψ production

[H. Mantysaari and A. Le - 2509.07480]

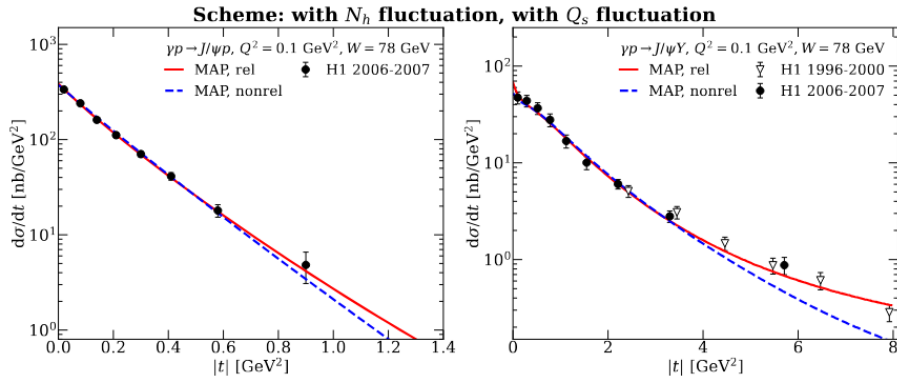
- Cross section for exclusive J/ψ production.
- Consider coherent and incoherent mechanisms. Probe either the average of configurations $|\langle \text{tr } VV^\dagger \rangle|^2$ or the variance of the configurations $|\langle \text{tr } VV^\dagger \rangle|^2 - |\langle \text{tr } VV^\dagger \rangle|^2$.
- **Hot spot model** for the initial condition. No evolution, but can be implemented using JIMWLK or BK.



Meson production: Coherent vs incoherent in exclusive J/ψ production

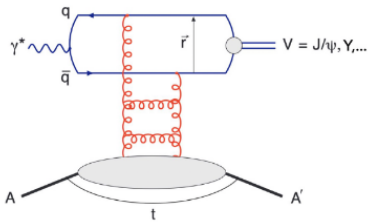
[H. Mantysaari and A. Le - 2509.07480]

- Cross section for exclusive J/ψ production.
- Consider coherent and incoherent mechanisms. Probe either the average of configurations $|\langle \text{tr } VV^\dagger \rangle|^2$ or the variance of the configurations $\langle |\text{tr } VV^\dagger|^2 \rangle - |\langle \text{tr } VV^\dagger \rangle|^2$.
- **Hot spot model** for the initial condition. No evolution, but can be implemented using JIMWLK or BK.



Exclusive heavy vector meson production: Gluon saturation at the LHC?

C. Royon and J. Penttala - Phys.Lett.B 864 (2025) 139394



- Heavy vector meson production in UPC at LHC. (proton or heavy ion target)
- γ -pomeron interaction: probe the low- x gluon distribution of the target.
- Gluon saturation? Probe with a low scale compared to Q_s , while perturbative.
- Low p_t for c or b production; or J/ψ production are ideal probes.

Calculation:

- BFKL or BK evolution.
- Impact parameter b -dependence in the dipole amplitude.
- Gaussian thickness for the proton / Wood-Saxon for heavy ion Pb .
- Adjusted BFKL to a fit of the vector meson data in the proton.

Exclusive heavy vector meson production: Gluon saturation at the LHC?

C. Royon and J. Penttala - Phys.Lett.B 864 (2025) 139394

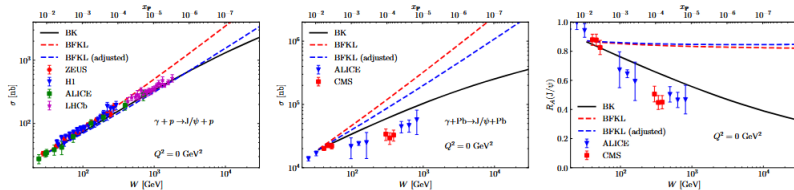


Figure 5: Exclusive J/ψ production as a function of the center-of-mass energy W . Left: Proton target, Center: Lead target, Right: Nuclear suppression factor,

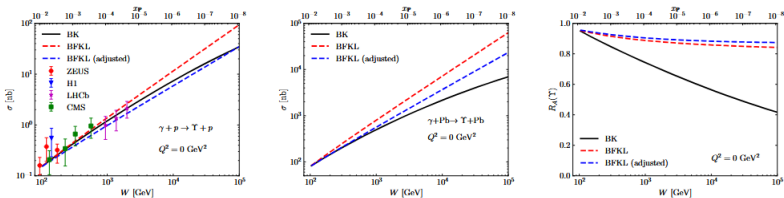


Figure 6: Exclusive Υ production as a function of the center-of-mass energy W . Left: Proton target, Center: Lead target. Right: Nuclear suppression factor.

Recap

Recap:

- Accuracy of CGC calculation has been improved by considering either NLO corrections or beyond eikonal approximation.
- Efforts are currently ongoing on unifying DGLAP and HE evolution
- Phenomenology for the EIC and LHC data is being considered by the community in a growing set of observables within the CGC framework.